Author Manuscript

Author Manuscript

Author Manuscript

Author Manuscript

HHS Public Access

Author manuscript

J Phys Chem B. Author manuscript; available in PMC 2016 June 04.

Published in final edited form as:

J Phys Chem B. 2015 June 4; 119(22): 6502–6515. doi:10.1021/jp5126415.

The Sensitivity of Non-Uniform Sampling NMR

Melissa R. Palmer, **Christopher L. Suiter**[a], **Geneive E. Henry**[b], **James Rovnyak**[c], **Jeffrey C. Hoch**[d], **Tatyana Polenova**[a], and **David Rovnyak**

Bucknell University, Dept. Chemistry, Lewisburg PA 17837

[a]Dept. Chemistry and Biochemistry, University of Delaware, Newark, DE 19716

[b]Dept. Chemistry, Susquehanna University, Selinsgrove, PA 17837

[c]Dept. Mathematics, University of Virginia, Charlottesville, VA 22904

[d]Dept. Of Molecular Biology and Biophysics, University of Connecticut Health Center, Farmington, CT 06030

Abstract

Many information rich multi-dimensional experiments in nuclear magnetic resonance spectroscopy can benefit from a signal-to-noise ratio (SNR) enhancement up to about two-fold if a decaying signal in an indirect dimension is sampled with nonconsecutive increments, termed non-uniform sampling (NUS). This work provides formal theoretical results and applications to resolve major questions on the scope of the NUS enhancement. First, we introduce the NUS Sensitivity Theorem, that *any* decreasing sampling density applied to *any* exponentially decaying signal always results in higher sensitivity (SNR per square root of measurement time) than uniform sampling (US). Several cases will illustrate this theorem, and show that even conservative applications of NUS improve sensitivity by useful amounts. Next, we turn to a serious limitation of uniform sampling: the SNR by US decreases for extending evolution times, and thus total experimental times, beyond 1.26 T_2 (T_2 = signal decay constant). Thus SNR and resolution cannot be simultaneously improved by extending US beyond 1.26 T_2. We find that NUS can eliminate this constraint, and introduce the Matched NUS SNR Theorem: an exponential sampling density matched to the signal decay always improves the SNR with additional evolution time. Though proved for a specific case, broader classes of NUS densities also improve SNR with evolution time. Applications of these theoretical results are given for a soluble plant natural product and a solid tripeptide (u-^{13}C,^{15}N-MLF). These formal results clearly demonstrate the inadequacies of applying US to decaying signals in indirect nD-NMR dimensions, supporting broader adoption of NUS.

Graphical Abstract

Correspondence to: David Rovnyak.

Author Manuscript Author Manuscript Author Manuscript Author Manuscript

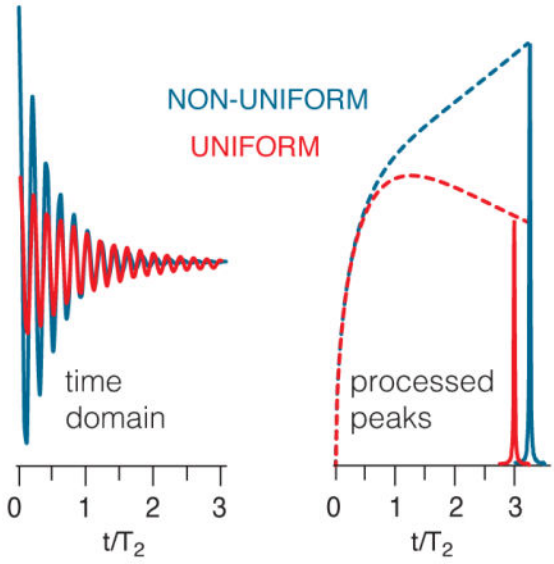

Keywords

nuclear magnetic resonance (NMR); nonuniform sampling; time domain signal to noise ratio; maximum entropy reconstruction; natural products NMR; biosolids NMR

Introduction

A growing practice for acquiring data in indirect evolution periods in NMR spectroscopy is non-uniform sampling (NUS), which often means acquiring data points (samples) in the time domain in non-consecutive time increments.[1,2] Traditionally, indirect evolution periods are recorded with equally spaced time increments, termed uniform sampling (US). Uniform sampling is paired with the Fourier Transform to obtain frequency domain signals, whereas NUS data can be treated with a number of robust non-Fourier algorithms for estimating frequency spectra.[3] Given that resolution is inversely proportional to evolution time, achieving long evolution times beyond T_2 is desirable in many applications of nD-NMR. Each sample in the indirect time dimension of nD-NMR is a specific time increment that is acquired as a one-dimensional (1D) experiment, with a certain number of transients for coherence selection. Uniform sampling must employ many incremented 1D-NMR experiments to reach evolution times that achieve needed resolution along the indirectly detected frequency axes. When recording decaying signals by US, it is a concern that long experiment times are devoted to samples that negligibly add to the signal-to-noise ratio ($T_2 < t < 1.26\ T_2$) or which decrease SNR ($t > 1.26\ T_2$).[4–6] In these cases, SNR is harmed by US in order to achieve resolution. For this reason, certain nD-NMR spectra may be out of reach for mass-restricted samples such as natural products and biosolids.[7,8] Improved signal-to-noise ratios in NMR spectra have been achieved through cryogenic probe circuitry, micro-coil probe heads, and dynamic nuclear polarization, but the fundamental SNR limitations on uniform sampling remain.

Author Manuscript Author Manuscript Author Manuscript Author Manuscript

Sculpting the acquisition to the signal envelope improves signal levels relative to noise.[1,9–11] Weighted non-uniform sampling (NUS) is the practice of acquiring a signal in proportion to its envelope (i.e. more data obtained where the signal is stronger) and yields SNR enhancements versus uniform sampling (US) for decaying signals.[1,7,12,13] Here, non-uniform sampling is implemented by choosing a weighting function to predetermine a list of samples (a sampling schedule) selected from the uniform grid, acquiring the same number of transients per sample, and specifying more samples where the signal has its highest intensity.[1] The SNR enhancement obtained by NUS is analytically solved and under user control,[7,12] although current NMR data acquisition software does not include facilities to compute this enhancement. Briefly, the NUS-based enhancement for sampling decaying signals can be understood in two parts. First, NUS eliminates many samples from evolution times after 1.26 T_2, where T_2 is the signal decay constant. Since all samples after 1.26 T_2 decrease the SNR of the raw data,[6] the SNR is improved when samples after 1.26 T_2 are eliminated. Second, the experimental time saved by not acquiring certain samples is used to acquire more transients across the weighted sampling schedule. In this report, NUS means the samples are selected from the Nyquist grid and are each acquired with the same number of transients, but NUS has been further generalized with respect to sample phases,[14] while a strategy of acquiring different numbers of transients on the uniform grid[10] has been revisited.[15,16]

Uniform sampling is governed by the Nyquist Theorem, which guarantees that signals in a certain frequency window will be correctly detected for a corresponding time interval between the acquired samples. Further, when US is paired with the Fourier transform, Parseval's Theorem guarantees that the frequency and time domain data have equal power or, stated informally, that the frequency domain signal produced by the FFT is a lossless representation of the uniformly acquired time domain data. Even as NUS is seeing wider adoption for acquiring the indirect dimensions of nD-NMR spectra, there is less theoretical support for the performance of nD-NMR by NUS compared to the formal results on US FT-NMR.

Bandwidth[17,18] and power[19–21] have been described previously for NUS. The frequency bandwidth of NUS is complicated and is not governed by Nyquist, but a great deal is known about the relative advantages of choosing the non-uniform points off the Nyquist grid[17] or on the Nyquist grid.[18] In either case, the concern is to minimize aliasing effects within the spectral window. These aliasing effects are reduced whenever the greatest common divisor (GCD) of the sample intervals is also reduced. For off-grid NUS, there is the possibility to dramatically increase the bandwidth if the precision of the sample times is very small.[17] However on-grid NUS is a much more widespread practice, where the GCD is usually just the inverse of the Nyquist frequency, meaning that the Nyquist frequency is treated as an upper bound on the NUS bandwidth. It has been demonstrated for on-grid NUS that when the NUS schedules are not too sparse, but instead contain several dense tracts, then NUS yields a bandwidth closely approximated by Nyquist, and better bandwidth is obtained by choosing the NUS schedule from an oversampled Nyquist grid.[18]

Also, linearity has been investigated for some reconstruction algorithms including maximum entropy reconstruction (MaxEnt). For example a maximum entropy interpolation regime

Author Manuscript Author Manuscript Author Manuscript Author Manuscript

(MINT) shows high linearity,[7] while MaxEnt is extremely useful in the non-linear regime.[19,22] Specifically, the MINT regime is useful when amplitudes need to be quantified or line shapes preserved, whereas the Bayesian regime where MaxEnt is non-linear is statistically robust. Whereas the bandwidth of NUS appears to depend most strongly on the choice of samples, the degree of linearity obtained by NUS is seen to depend on both the sampling schedule and the method of spectral estimation, suggesting that it may be difficult to characterize power conservation based only on the NUS schedule alone. Although NUS-MaxEnt is employed here, there are a number of non-traditional approaches to nD-NMR and subsequent spectral estimation, which are recently reviewed.[23] A few highlights of recent developments include time resolved nD-NMR using NUS combined with multi-way decomposition,[24] and new efficient algorithms for l1-norm regularization.[25] In addition, compressed sensing,[26,27] and soft thresholding,[28,29] are finding wider use in biomolecular applications, while unsymmetrical covariance has shown high promise in unraveling natural products spectra.[30,31]

This report characterizes the signal-to-noise ratio (SNR) in the time domain, a strategy which has been shown to have high utility because it avoids the problems attending nonlinearity of most non-Fourier methods for estimating the spectrum.[4,6] Time domain calculations assuming continuous functions for the signal and sampling density are convenient for describing NUS. In general, a great deal of time domain analytic results can be obtained with formal theory.[4,6] Specifically, it has been shown for time-domain NUS SNR calculations that theoretical predictions based on continuous functions correspond well to calculations and experiments using discrete NUS schedules, as long as the discrete NUS schedule follows its prescribed density reasonably closely.[12] Additionally, the time domain SNR describes fundamental properties of the non-uniform samples themselves, prior to and independent of any and all subsequent data manipulations and transforms. Indeed, it is useful from this point on to distinguish the signal-to-noise ratio of the raw data prior to post-acquisition manipulations as the *intrinsic* SNR, or *i*SNR.[32] Any improvement in the *i*SNR of the acquired time domain data is then available to subsequent spectral reconstruction techniques, regardless of whether they are linear or not. Since a variety of computational techniques can be used to increase the apparent SNR starting from the *i*SNR, we recognize that the *i*SNR is a fundamental constraint on detecting a peak, and thus a peak is intrinsically more detectable if its *i*SNR is improved. The importance of improving *i*SNR is embodied in hardware advances such as DNP and cryogenically cooled probes whose sole effect is to improve the *i*SNR of the time domain data, which of course lead to improved peak detection. Non-uniform sampling a decaying signal following a weighting function increases the *i*SNR, and the NUS *i*SNR enhancements that have been measured using a linear transform, maximum entropy interpolation, agree closely with theoretical predictions of NUS *i*SNR enhancements in the time domain.[7]

We report here two theorems that govern the *i*SNR of non-uniform sampling applied to decaying signals. First, it is shown that NUS always has greater *i*SNR than US in the same experimental time, and thus greater sensitivity, when using *any* decreasing NUS density. This is a very broad rule, which we term the NUS Sensitivity Theorem. Next, we address a question that has been overlooked to date: given that uniform sampling has an *i*SNR maximum at an evolution time of about 1.26 T_2,[4,6] are there similar maxima for NUS that

Author Manuscript Author Manuscript Author Manuscript Author Manuscript

could guide experimentalists in designing NUS experiments? A perhaps surprising finding follows: we prove in a second theorem that, for matched exponential NUS, the *i*SNR is always increasing with evolution time and has no maximum. Although proved for the narrow case of matched exponential NUS, we employ a simple graphical strategy to verify that many useful NUS densities have this property of a positive *i*SNR slope at all evolution times. We term this second result the Matched NUS SNR Theorem; it has a remarkable interpretation: given that increasing evolution time increases the ability to resolve signals, any NUS density with increasing *i*SNR at all times has the distinction of *simultaneously increasing* i*SNR and resolution with additional evolution time*, a statement that is not true for uniform sampling. With these stronger theoretical insights on the fundamental properties of raw NUS data, wider adoption of weighted NUS for detecting decaying signals in indirect dimensions of nD-NMR is merited.

Theoretical Results

(i) Theorems for the Sensitivity and SNR of Non-Uniform Sampling

As noted above, the *intrinsic SNR* (*i*SNR) of the raw data prior to post-acquisition manipulations is distinguished from the *apparent SNR* of data following manipulations such as apodization, linear prediction, etc.[32] Once the receiver is turned off, the *i*SNR is fixed. Although spectra can be produced with apparent SNR greater than the *i*SNR, the apparent SNR is constrained by the original signal. If a power conserving transform, such as the Fourier transform, is used as the sole post-acquisition operation on the data, then the *i*SNR is equal in the time and frequency domains. The SNR of non-Fourier reconstructed spectra may not be a valid metric,[33] but the time domain *i*SNR is (i) a processing-independent metric of signal strength relative to noise, and (ii) not subject to folding artifacts, which are viewed as sampling noise.[18,34] We will see shortly that *i*SNR is also independent of the implementation of NUS, so that it is a general metric for describing NUS. The method of spectrum analysis used to convert time-domain data into frequency-domain spectra also impacts the sensitivity, and with the emergence and importance of nonlinear non-Fourier methods for dealing with NUS data, this is a nontrivial problem. Focusing on iSNR allows us to isolate these impacts from the impact of the amount of signal captured by a sampling strategy. This report analyzes and compares solely the *i*SNR of uniform and non-uniform sampling, but some results here could apply also to the apparent SNR.

An exponentially decaying signal with an arbitrary positive T_2 value is assumed in all further analysis. It is convenient to take the signal to be at zero frequency so that it is described only by its decay, $S(t) = e^{-t/T_2} = e^{-tR_2}$, where $R_2 = 1/T_2$, and normally one considers the net decay T_2^*. The time domain *i*SNR is the ratio of the integral of the signal envelope to the square root of the signal evolution time.[4,6,22,35] For US, the dependence of the *i*SNR on evolution time is[4,6]

$$i\mathrm{SNR}(t) \propto \frac{1-e^{-tR_2}}{R_2\sqrt{t}}. \quad (1)$$

Author Manuscript Author Manuscript Author Manuscript Author Manuscript

For a power conserving transform such as the Fourier transform, the definition of SNR in the time domain is equivalent to the familiar definition of SNR in the frequency domain as the ratio of the peak height, $S(\omega)$, to the rms noise. Briefly, the square root of the signal evolution time is proportional to the rms noise in the frequency domain, and the integral of the signal envelope is the peak height when employing the power conserving Fourier transform.[4,6] Recalling that sensitivity is the SNR per square root of experimental time,[36] the terms SNR and sensitivity are interchangeable when comparing experiments that consume equal times. Equation (1) has several implications for uniform sampling.[1,4] The maximum SNR occurs for $t_{max} \sim 1.26\ T_2$ (Figure 1A), which falls short of the $\sim 3 T_2$ evolution time needed to obtain optimal resolution (Figure S.1 and citations therein). Thus, US can improve either SNR ($t < 1.26\ T_2$) or resolution ($t \sim 3\ T_2$), each at the expense of the other.

Some further notation follows next. Non-uniform sampling an exponentially decaying signal using an exponential density of samples will be termed exponential NUS. Matched exponential NUS means the decay constant of the NUS probability density (T_{SMP}) equals that of the signal (T_2). Biased NUS takes more samples at early signal evolution times than matched NUS, meaning $T_{SMP} < T_2$ in the case of exponential NUS. Exponential and Gaussian sampling densities are straightforward to modify for biased NUS. For example, we often treat the case of a sampling density with a decay rate that is twice that of matched NUS, and call this case two-fold biased NUS (Figure 1bc). Next we briefly review prior results (Eqs. 1–6).

Non-uniform samples are chosen according to a probability density, $h(t)$, a function which prescribes the likelihood that a sample will be recorded at a given evolution time, t. To guarantee that uniform and non-uniform sampling consume identical experimental times, their sampling densities must have equal areas. Setting uniform sampling to have a constant probability density of 1, and letting $h(t)$ be the NUS density, then[12]

$$\chi(t_{max}) = \frac{t_{max}}{\int_0^{t_{max}} h(t)dt} \quad (2)$$

is the scaling factor which guarantees that NUS and US use equal total experiment times. For matched exponential NUS,

$$\chi_{match\text{-}exp} = \frac{\alpha_{max}}{1 - e^{-\alpha_{max}}}, \quad (3)$$

where the total signal evolution t_{max} can be parameterized as $\alpha_{max} = t_{max}/T_2$. Taking $S(t) = e^{-t/T_2}$ as the signal envelope, the uniform signal is scaled by unity, while the NUS signal is $\chi h(t) S(t)$. In other words, χ describes a simple experimental protocol in NUS which can be illustrated by example: suppose a uniform acquisition employs 2 transients for each of 512 incremented evolution times; then a NUS schedule which selects one quarter of these would employ 8 transients for each of the 128 samples selected from the original Nyquist grid.

Author Manuscript Author Manuscript Author Manuscript Author Manuscript

Notice that these and all subsequent results depend only on the probability density $h(t)$, regardless of how the experimenter implements $h(t)$. The sampling density $h(t)$ could be realized by different numbers of transients on a uniform grid, by selecting samples non-uniformly from a uniform grid or off-grid, by random phase methods, and by a combination of these approaches. Consider also that different randomly generated lists of samples could all closely conform to a given $h(t)$. In other words, all of the results in this manuscript for the *i*SNR are sampling-independent, meaning they apply to any method of acquiring data following a weighting function $h(t)$.

If NUS and US acquisitions use the same experimental time, they must employ the same number of transients and therefore have the same noise, which means that it is only necessary to compare the amount of signal recorded by NUS and US to determine *i*SNR enhancements. The NUS-based *i*SNR enhancement is obtained as the ratio of the non-uniform and uniform signal areas,

$$\eta=\frac{\chi\left(t_{\max}\right)\int_0^{t_{\max}}h(t)e^{-t/T_2}\,dt}{T_2\left(1-e^{-\alpha}\right)}=\frac{\alpha}{\left(1-e^{-\alpha}\right)}\frac{\int_0^{t_{\max}}h(t)e^{-t/T_2}\,dt}{\int_0^{t_{\max}}h(t)dt}, \quad (4)$$

which is general for any sampling density $h(t)$.[7] For exponential NUS, equation (4) becomes

$$\eta_{\exp}=\frac{\chi\left(1-e^{-\alpha\left(\left(T_2/T_{SMP}\right)+1\right)}\right)}{\left(T_2/T_{SMP}+1\right)\left(1-e^{-\alpha}\right)}. \quad (5)$$

For matched exponential NUS, the enhancement is

$$\eta_{\text{match- exp}}=\frac{\chi\left(1-e^{-2\alpha}\right)}{2\left(1-e^{-\alpha}\right)}=\frac{\alpha}{2}\frac{\left(1+e^{-\alpha}\right)}{\left(1-e^{-\alpha}\right)}. \quad (6)$$

The *i*SNR enhancements (η) for matched and two-fold biased exponential NUS relative to uniform sampling in the same total experimental time are illustrated in Figure 1b, and can approach or slightly exceed a factor of two, respectively.[12] Theory and linear reconstructions of experimental NUS data show close agreement, and also that improving the *i*SNR by NUS enables detecting new peaks.[7,12,37] Further, applying NUS in multiple indirect dimensions compounds the *i*SNR enhancements up to about four-fold.[7,37] The key conditions for realizing an NUS-based *i*SNR enhancement are that the signal must have a decreasing amplitude envelope, and the NUS must follow a probability density that favors the signal envelope. It is not possible to obtain NUS-based *i*SNR enhancements for constant-time evolution periods or by random (i.e. unweighted) sampling.[12]

Equations 1–6 have been reported,[12,20] and visual inspection suggests that the enhancement for matched exponential NUS represented in Figure 1b appears to always be greater than one. Could NUS ever decrease the *i*SNR relative to US in the same time? This question can be answered very generally, that a NUS-based *i*SNR enhancement is always greater than one for *any* non-constant sampling density applied to *any* exponentially decaying signal

Author Manuscript Author Manuscript Author Manuscript Author Manuscript

(Appendix A1). A function $h(t)$ defined on an interval is called nonincreasing if $h(t_1) \geq h(t_2)$ for any points $t_1 < t_2$ in the interval.

Theorem I (NUS Sensitivity Theorem). Assume $h(t)$ is a positive, nonincreasing function on some interval $0 \leq t < A$, where $A \leq \infty$. For any positive T_2 and $0 < t_{max} < A$, the time domain *i*SNR enhancement (Eq. 4) satisfies

$$\eta = \frac{\alpha}{(1-e^{-\alpha})} \frac{\int_0^{t_{max}} h(t) e^{-t/T_2}\, dt}{\int_0^{t_{max}} h(t) dt} \geq 1, \quad \text{(A1)}$$

where $\alpha = t_{max}/T_2$, and equality holds if and only if $h(t)$ is constant for $0 < t < t_{max}$.

Since Theorem 1 treats the *i*SNR of NUS and uniform experiments using equal experimental times, it therefore assures that the use of any decreasing sampling density results in greater *sensitivity* than uniform sampling. As one practical example, it can be appreciated from Figure 1b that the sensitivity advantage for exponential NUS is negligible for short evolution times but is nontrivial for times beyond T_2, which will be seen to be a theme for other NUS densities as well. The enhancements for several other sampling densities will be computed in the next section to demonstrate the broad applicability of Theorem 1 to a variety of decreasing sampling densities.

Theorem 1 applies to both continuous and discontinuous NUS densities such as step functions, which have been used to good effect in prior work.[7] Notice also that Theorem 1 establishes that equal sensitivity for US and NUS holds only if the NUS density is constant, which would be the case for a random non-uniform sampling density. A special case of constant sampling density is a comparison of 2D-HSQC spectra obtained with different spectral windows, for which *i*SNR is not changed. (Figure S.1,[12]).

Another key question has yet to be considered: how does the *i*SNR of NUS depend on the evolution time? In other words, by analogy to the 1.26 T_2 *i*SNR maximum for uniform sampling, is there also an *i*SNR maximum in the time evolution of NUS? To learn the *i*SNR of exponential NUS (Figure 1c), the *i*SNR of uniform sampling (Eq. 1, Figure 1a) is scaled by the NUS-based enhancement (Eq. 5, Figure 1b), giving

$$i\mathrm{SNR}_{\mathrm{exp}} \propto \frac{T_2 \sqrt{t}}{(T_2 + T_{\mathrm{SMP}})} \frac{(1-e^{-\alpha((T_2/T_{\mathrm{SMP}})+1)})}{(1-e^{-\alpha T_2/T_{\mathrm{SMP}}})}. \quad \text{(7a)}$$

For matched NUS, $T_2 = T_{SMP}$, a simpler form emerges:

$$i\mathrm{SNR}_{\mathrm{match\text{-}exp}} \propto \frac{(1+e^{-\alpha})\sqrt{t}}{2}. \quad \text{(7b)}$$

Inspection of Figure 1c suggests that the *i*SNR by NUS is always increasing with evolution time; in other words there appears to be no time that gives a maximum *i*SNR in matched or biased (e.g. $T_2/T_{SMP} = 2$) NUS. Confirming our visual inspection of the NUS curves in

Author Manuscript Author Manuscript Author Manuscript Author Manuscript

Figure 1c, it can be proved that Equation (7b) is always increasing with evolution time (Appendix A2):

> **Theorem 2 (Matched NUS SNR Theorem)**: The *i*SNR of matched exponential NUS (Equation 7b) always has a positive slope for an arbitrary, positive T_2 and positive evolution time t_{max}.

Although Theorem 2 is proved for the case of matched exponential NUS, it is appreciated by inspection of Figure 1c for example, that any biased ($T_{SMP} < T_2$) exponential NUS density also has the property of a positive *i*SNR slope for all times. Specifically, it will be shown empirically that the *i*SNR has a positive slope at all times for exponential densities for which $T_{SMP}/T_2 > 1.35$, encompassing a broad class of useful NUS densities. Some decreasing NUS densities do not improve *i*SNR slope for all times, so Theorem 2 may not be stated for all decreasing NUS densities. Analytic expressions for the *i*SNR of several other NUS densities will be given and evaluated visually to verify that the conclusions of Theorem 2 do hold for other large classes of useful sampling densities. Since uniform sampling has a decreasing *i*SNR beyond 1.26 T_2, Theorem 2 is certainly not true for uniform sampling. *An important restatement of Theorem 2 is possible,*

> Matched exponential NUS simultaneously improves resolution and *i*SNR if increased experimental time is used to span longer evolution times of a decaying signal.

Acquiring samples at longer evolution times non-uniformly will introduce more constraints on distinguishing closely spaced signals and will improve resolution.[32] While resolution is inversely proportional to evolution time for US, there is not an analytic rule to describe by how much the resolution improves with NUS evolution time. Empirically, matched NUS has been shown to yield resolution comparable to uniform sampling when they span the same evolution period and when the degree of data reduction is on the order of a third to a fourth of the US samples.[7,12,32] On the other hand, strongly biased NUS (e.g. $T_2/T_{SMP} \geq 2$), does not yield the same resolution as uniform sampling over the same evolution time and the increase in signal resolution with evolution time by biased NUS is complex and needs more investigation.[7,8,32]

Theorem 2 can only be stated with respect to the *i*SNR. Sensitivity does not have a positive slope with evolution time by NUS or US. Recall that sensitivity is SNR per square root of experimental time. Evolution time is directly proportional to experimental time, so that the intrinsic sensitivity of NUS is obtained by dividing equation 7b by the square root of time, giving

$$\text{Sensitivity}_{\text{match- exp}} \propto (1+e^{-\alpha}), \quad (7c)$$

where the factor of 2 is dropped since this is already a proportionality, and it is seen that equation 7c is clearly a decreasing function with evolution time. Sensitivity also decreases with evolution time for US (equation 1 divided by the square root of time),

Author Manuscript Author Manuscript Author Manuscript Author Manuscript

$$\text{Sensitivity}_{\text{uniform}} \propto \frac{1}{t}(1-e^{-\alpha}), \quad (8)$$

where it can be recognized that *sensitivity by matched exponential NUS decreases at a slower rate than the decrease in sensitivity by uniform sampling*.

In principle, the signal is continuously sampled following the NUS probability density, however signals are sampled discretely, and an NUS schedule is a list of the time domain samples in which more are acquired where the probability density is greater. The close correspondence between discrete and continuous treatments is further demonstrated by sensitivity results reported using discrete treatments which include confirming well known results such as the 1.26 T_2 limit.[38] Prior work has shown that the degree to which a discrete NUS schedule conforms to the desired density influences if the theoretical NUS enhancement is realized, that significant *t*SNR enhancements are obtained even when NUS schedules follow an exponential sampling density coarsely, and that typical and conservative applications of NUS closely approach the theoretical predictions for the *t*SNR enhancement.[7,12] In other words, the properties of Theorem 2 therefore apply to diverse discrete implementations of NUS.

It is technically correct that, as illustrated in Figure 1c, an arbitrary *t*SNR improvement by NUS versus US occurs for evolution times beyond πT_2, but two cases need to be clarified. First, if all signals have similar relaxation rates, the high NUS enhancements for $t_{max} \gg \pi T_2$ derive from eliminating samples containing only noise ($>\pi T_2$) and replacing them with samples containing signal ($<\pi T_2$), an unfair comparison to US. When T_2 values are uniform, sampling beyond πT_2 by US or NUS is not justified. A second case is if signals have a distribution of T_2 values. Then an exponential NUS density at the average of the T_2 values causes the enhancements of the faster and slower decaying signals to be closer to the enhancement for the $T_{2,\text{avg}}$ value. For example, large enhancements are not realized for faster decaying signals ($t_{max} \gg \pi T_{2,\text{fast,}}$) since the NUS density favors the slower $T_{2,\text{avg}}$. When T_2 varies over an order of magnitude, a narrow range of enhancements is observed.[39]

We tested Eqs. 7a–7b by performing simulations in which a noise FID received injected signals corresponding to non-uniformly distributed transients on a uniform grid, having the same sampling density as NUS,[10] but treatable by the power-conserving fast-Fourier transform (FFT). The FFT of matched (Eq. 7b) and two-fold biased (Eq. 7a) exponential sampling confirms theoretically predicted NUS signal intensities.(Figure 2). Again, equations 7a–b and Figure 2 are presented so that increasing evolution time entails greater overall experimental time. Taking an experiment from $1T_2$ to $3T_2$ will significantly improve resolution but will also require threefold more experiment time, which would harm *t*SNR by US, but is seen to increase *t*SNR by NUS. The strong positive slope of the NUS *t*SNR peak intensities in Figure 2 confirms Theorem 2.

For further experimental confirmation, recently reported data[32] also provide an example of how NUS *t*SNR enhancements are governed by Eqs. 7ab, included here in the supporting information (Figure S2). Compounding the NUS-based *t*SNR enhancement (equation 5) in multiple dimensions yields enhancements on the order of three- to fourfold, which was

Author Manuscript Author Manuscript Author Manuscript Author Manuscript

experimentally observed in biosolids applications.[7] By analogy, the direct calculation of *i*SNR in Eqn. 7a can be compounded for two NUS dimensions (Figure 3), to help illustrate how *i*SNR depends on time in two indirect evolution periods. First, recall that the highest obtainable *i*SNR by US is achieved if each evolution period is sampled to 1.26 T_2 and that iSNR by US decreases for longer evolution times (e.g. the US curve in Figure 2). Thus, when employing US in two indirect evolution periods, the *i*SNR after 1.3 T_2 now *decreases at a compounded rate* (Figure 3a, obtained compounding the US curve in Figure 2). In contrast, *iSNR by NUS increases at a compounded rate* for longer evolution times in multiple dimensions (Figure 3bc).

Finally, it should be stressed that Theorems 1 and 2 apply equally to on-grid NUS, non-uniform transients on the uniform grid (eg Figure 2),[10,15,16] off-grid NUS, hypercomplex NUS,[14] and other implementations that may yet arise.

(ii) Analyses of other Sampling Densities

A survey of the *i*SNR performance of several NUS densities follows, placing each in context with Theorems 1 and 2. These are sinusoidal, Gaussian, linear and cosine weighted NUS. Graphical inspection is particularly useful in recognizing how the properties of these NUS densities relate to Theorems 1 and 2.

Sinusoidal NUS Density—The portion of the sine between π and 3π/2 has recently been investigated as an alternative to the matched exponential NUS density, where it was found to have a nearly identical *i*SNR enhancement to that of matched exponential NUS, while also yielding improved constraints on line shapes.[32] The *i*SNR of this sinusoid will be analyzed by equations 2, and 4. The sampling density prior to normalizing its area versus uniform sampling is

$$h(\text{sinusoid},t)=1-\sin\left(\frac{t}{\pi T_2}\frac{\pi}{2}\right)=1-\sin\left(\frac{t}{2T_2}\right), \quad (8a)$$

which spans an acquisition time of πT_2. Equation 2 is employed to find the scaling factor that normalizes the sinusoidal density to have the same area as the uniform density,

$$\chi(\text{sine})=\frac{t_{\max}}{\int_0^{t_{\max}}(1-\sin(\frac{t}{2T_2}))dt}=\frac{\alpha}{\alpha+2[\cos(\frac{\alpha}{2})-1]}, \quad (8b)$$

where $\alpha = t_{\max}/T_2$, and the resulting density is illustrated in Figure 4a. Now the *i*SNR enhancement for sinusoidal NUS is determined,

$$\eta(\text{sine})=\frac{\chi(\text{sine})\int_0^{t_{\max}}(1-\sin(\frac{t}{2T_2}))e^{-t/T_2}\,dt}{T_2(1-e^{-t/T_2})},$$

which yields

Author Manuscript Author Manuscript Author Manuscript Author Manuscript

$$\eta(\text{sine},t)=\chi(\text{sine})-\frac{\chi(\text{sine})\times(2-4e^{-\alpha}(\sin\frac{\alpha}{2}+\frac{1}{2}\cos\frac{\alpha}{2}))}{5(1-e^{-\alpha})}, \quad (8c)$$

and is illustrated in Figure 4b. To calculate the *i*SNR for the sinusoidal NUS, Eq. 8c is multiplied by Eq. 1, and the result is illustrated in Figure 4c. As we could expect from observing the close agreement between the sinusoidal and matched exponential densities in Figure 4a, their respective *i*SNR values are very similar to each other. However the sinusoidal density does include more samples beyond $1T_2$ than a matched exponential density, yielding slightly improved line shapes in spectra obtained by MaxEnt processing.[32] Inspection of Figure 4b illustrates Theorem 1 for the sinusoid, that the enhancement is always greater than 1. Theorem 2 was proved for the specific case of matched exponential NUS, but inspection of Figure 4c shows that the *i*SNR using the sinusoidal NUS density also always has a positive slope with evolution time sinusoid.

Gaussian NUS Density—Let the NUS time domain weighting be

$$h(gauss,t)=e^{-t^2/2\sigma^2}, \quad (9a)$$

where σ is a constant to be determined. Consider the Fourier Transform of equation 9a,

$$h(\nu)=\frac{1}{\theta\sqrt{2\pi}}e^{-\nu^2/2\theta^2},$$

where $\theta\equiv 1/2\pi\sigma$ and the line width is $2\theta\sqrt{2\ln 2}$. In order for Gaussian NUS to be 'matched', the frequency domain line width (full width at half maximum) of the Gaussian NUS density must equal the line width of the signal decay, which is $1/\pi T_2$. One then finds that 'matched Gaussian' NUS is obtained when $\sigma^2=2T_2^2\ln 2$ is employed in Equation 9a. For an evolution time t_{max}, find the scaling factor according to Equation 2:

$$\chi\,(\text{Match- Gauss})=\frac{t_{\max}}{\int_0^{t_{\max}}e^{-t^2/4T_2^2\ln 2}\,dt}=\frac{t_{\max}}{T_2\sqrt{\pi\ln 2}\times erf(\alpha/2\sqrt{\ln 2})}, \quad (9b)$$

where, again, $\alpha = t_{max}/T_2$ is convenient for parameterizing the evolution time. Next compute the *i*SNR enhancement using Equation 4 and inserting the scaling factor just obtained for matched-guassian NUS in Equation 4:

$$\eta(\text{Match- Gauss})=\frac{\chi(\text{Match- Gauss})\int_0^{t_{\max}}e^{-t^2/4T_2^2\ln 2}e^{-t/T_2}\,dt}{T_2(1-e^{-t/T_2})}.$$

After completing the square in the exponent, the integral for the *i*SNR enhancement of matched Gaussion NUS simplifies to

Author Manuscript Author Manuscript Author Manuscript Author Manuscript

$$\eta(\text{Match- Gauss})=\frac{2\alpha}{erf\left(\frac{\alpha}{2\sqrt{\ln 2}}\right)}\frac{erf\left(\frac{\alpha+2\ln 2}{2\sqrt{\ln 2}}\right)-erf\left(\sqrt{\ln 2}\right)}{(1-e^{-\alpha})}. \quad (9c)$$

Similar to the sinusoid, the Gaussian density also acquires more samples after $1\,T_2$ than matched exponential NUS. The Gaussian density is a decreasing function and so the enhancement for Gaussian NUS must always be greater than 1 according to Theorem 1, which can be appreciated by inspection of Figure 4b. Finally, the *t*SNR is seen from Figure 4c to always increase with evolution time.

Linear NUS Density—A linearly decreasing sampling density is also capable of placing more emphasis on sampling early portions of the exponential signal. As will be seen, the linear density does not emphasize early evolution times as much as the matched exponential, sinusoidal and matched Gaussian densities. So the linear density is a very conservative choice for implementing NUS. Prior to normalization, the density is

$$h(t)=1-{}^{t}\!/_{\pi T_2}\,, \quad (10a)$$

which continues the practice herein to consider sampling densities spanning $\pi\,T_2$. The normalization factor computed from equation 2 is

$$\chi(\text{linear})=\frac{t_{\max}}{\int_0^{t_{\max}}\left(1-{}^{t}\!/_{\pi T_2}\right)dt}=\frac{1}{1-\frac{\alpha}{2\pi}}, \quad (10b)$$

where the linear density is seen to specify much greater sampling beyond $1\text{x}\,T_2$ than matched exponential NUS. The *t*SNR enhancement by linearly weighted NUS is

$$\eta=\frac{\chi(\text{sine})\int_0^{t_{\max}}\left(1-{}^{t}\!/_{\pi T_2}\right)dt}{T_2(1-e^{-\alpha})}=\frac{(1-e^{-\alpha})-\frac{1}{\pi}(1-(\alpha+1)e^{-\alpha})}{(1-e^{-\alpha})(1-{}^{\alpha}\!/_{2\pi})}. \quad (10c)$$

One can see by inspection of the figures that the linear density not only includes more sampling density after $1\,T_2$ than any of the densities in Figure 4, it also restores more samples after $2\,T_2$ than the sinusoid, Gaussian and matched-exponential. Figure 5b illustrates that the enhancement is still always greater than 1 as required by Theorem 1, but Figure 5c shows that the *t*SNR grows at a much slower rate than the densities in Figure 4.

Cosine NUS density—An even more conservative NUS approach is a probability density weighted according to the 0-π/2 portion of the cosine function. The cosine density will only weakly bias the early portion of the signal, and will retain even more samples beyond $1\times T_2$ than the linear density. Following the recipe that has been illustrated for the cases above, we first define the cosine density over the time period $\pi\,T_2$, prior to normalizing it against uniform sampling, as

Author Manuscript Author Manuscript Author Manuscript Author Manuscript

$$h\,(\text{cosine},t)=\cos\left(\frac{t}{\pi T_2}\frac{\pi}{2}\right)=\cos\left(\frac{t}{2T_2}\right). \quad (11a)$$

The normalizing factor for this cosine density is

$$\chi\,(\text{cosine})=\frac{t_{\max}}{\int_0^{t_{\max}}\cos\left(\frac{t}{2T_2}\right)dt}=\frac{\alpha}{2\sin\frac{\alpha}{2}}, \quad (11b)$$

leading to the *I*SNR enhancement for cosine weighted NUS as

$$\eta=\frac{\alpha}{10\sin\left(\frac{\alpha}{2}\right)\left(1-e^{-\alpha}\right)}\left(4+2\sin\frac{\alpha}{2}e^{-\alpha}-4\cos\left(\frac{\alpha}{2}\right)e^{-\alpha}\right). \quad (11c)$$

As NUS densities more closely resemble uniform sampling, it is to be expected that their *I*SNR enhancements will decrease further, as seen here with the cosine density. Still, the cosine density is a decreasing function, and so Equation 11c is governed by Theorem 1. Indeed, inspection of Figure 5b confirms that all enhancements are greater than 1.

By graphical inspection, it has been seen for the other densities considered above that they all exhibit an *I*SNR with a positive slope for all evolution times. However the cosine density is interesting because, as shown in Figure 5c, its *I*SNR is approximately constant for a broad range of evolution times (about $1\,T_2 - 2.5\,T_2$). So the cosine density may not have the properties of Theorem 2.

(iii) Scope of Theorem 2

The properties of the cosine density illustrate that it is possible to choose very conservative NUS densities which may not have increasing *I*SNR with evolution time (Figure 5). Whereas Theorem 1 applies broadly to any sampling density that is nonincreasing, Theorem 2 has a narrower scope, which should be characterized further. We return to the exponential and Gaussian sampling densities, since it is straightforward to modify them to sample more densely at early or later times.

It is useful to introduce the ratio of the line width of the sampling density to the line width of the signal, or LW_{SMP}/LW_{sig}. As explained in the prior sections, we say that the NUS exponential or Gaussian density is 'matched' if $LW_{SMP}=LW_{sig}$. If we choose to bias the NUS to acquire more data at earlier times relative to matched NUS, then we are specifying $LW_{SMP} > LW_{sig}$. For example, the case of $LW_{SMP}/LW_{sig}=2$ is often referred to informally as 2X biased NUS, and can result in *I*SNR enhancements over two-fold.[7,12] The time dependence of the *I*SNR for different LW_{SMP}/LW_{sig} ratios is obtained by equations 2, 4 and 7, as illustrated in Figure X6. It is seen through inspection that the exponential NUS density will have a positive *I*SNR slope at all times if $LW_{SMP}/LW_{sig} > \sim 0.35$, while the Gaussian NUS density will deliver positive *I*SNR slopes at all times for $LW_{SMP}/LW_{sig} > \sim 0.60$ (Figure 6). Matched exponential and Gaussian NUS (e.g. $LW_{SMP}/LW_{sig} \sim 1.0$) are already viewed as rather conservative on the basis of extensive experimentation. The NUS densities illustrated with black lines in Figure 6 have negative *I*SNR slopes, similar to uniform sampling, but

Author Manuscript Author Manuscript Author Manuscript Author Manuscript

correspond to situations that are unlikely to be used in NUS practice. Indeed, it would be straightforward to modify NUS acquisition software to advise users on whether they are in the positive or negative *i*SNR slope regimes.

Experimental Results

We tested the theoretical results and simulations of the prior section first with 2D HSQC spectra of a plant-derived natural product that has ^{13}C line widths ca. 3.7 Hz (T_2*~86 ms, 25°C, DMSO). The ^{13}C dimension must span 265 ms (~3.1 T_2, Figure S.1) to obtain this line width. First, the potential to use NUS to improve the spectra for an evolution time spanning 1.3 T_2 is considered in Figure 7. Comparing Figure 7b and 7c, there is only a slight gain in spectral quality from applying matched exponential NUS to a maximum evolution time of 1.3 T_2. Some improvement results from using two-fold biased NUS (Figure 7a and 7c) at 1.3 T_2. The data in Figure 7 are adjusted such that the uniformly sampled data, processed by FFT, is at the limit of detection for most peaks, by mis-setting the proton pulse width. It has been a concern that the use of spectral reconstruction methods could be misleading as they improve the apparent SNR.[33] Yet Figure 7 clearly shows that neither the slight improvement in *i*SNR by NUS nor the use of MaxEnt can significantly change the detectability of peaks when evolution times span about 1.3 T_2, although two-fold biased NUS does show some slight improvement in signal detection. In contrast, substantial enhancements are observed by NUS when the evolution time spans about 3T_2. In Figure 8, uniform and exponential NUS data are compared for a maximum evolution time of about 3T_2, where significant improvements by NUS are realized. Both ^{1}H and ^{13}C cross-sections verify the significant gains. Importantly, contrasting Figure 7–8 leads to the realization that the improvement illustrated in Figure 8 must owe to changing the iSNR of the raw data by NUS, and not to the use of MaxEnt. Indeed, these experiments used conditions in which the MaxEnt reconstruction approaches linear behavior, so that the ^{13}C cross-sections show close agreement with theoretical predictions (Figure 8, top). The agreement between the ^{13}C cross-sections and the theory is not exact since the peak heights have uncertainty from the high level of noise, and also because the reconstruction by MaxEnt was not perfectly linear. In the next section, results from the formally linearized protocol for maximum entropy, termed MINT,[20] will also be shown.

Contrasting NUS evolution to 1.3T_2 and 3T_2 in Figure 7–8 confirms both key theorems developed herein. We see that, following Theorem 1, all exponential NUS cases resulted in greater SNR than uniform sampling. Next, following Theorem 2, the positive iSNR slope with evolution time is illustrated by recognizing the much larger NUS-based enhancements were realized for 3 T_2 than for 1.3 T_2. MaxEnt processing is not responsible for the trends observed here: consider that the improved spectral quality of the biased versus matched NUS (e.g. Figure 8ab) must owe to higher *i*SNR in the time domain of the biased NUS data since both were processed with identical maximum entropy reconstruction (MaxEnt) parameters. That is, MaxEnt is not responsible for *i*SNR enhancements.[33]

We also examined 2D ^{13}C-^{13}C homonuclear correlation spectroscopy of biological systems under magic angle spinning (MAS), posing unique challenges: i) high dynamic range with signal intensities spanning over two orders of magnitude; ii) a spread of T_2* values over an

Author Manuscript Author Manuscript Author Manuscript Author Manuscript

order of magnitude from 1–30 ms in the same sample (even longer T_2* values with fast-MAS methods). The latter mandates sampling to long t_1 evolution times to attain high resolution, particularly in large protein assemblies exhibiting narrow lines.[39] Indeed, NUS is ideally suited to these conditions, and conservative NUS schemes paired with MINT processing produce high-quality artifact-free spectra with sensitivity gains consistent with theory.[7,39] In the U-^{13}C,^{15}N-MLF tripeptide the average T_2* relaxation time is 3 ms, and the longest is ca. 10.8 ms (methyl Cδ of met).

The average T_2* is very short: to avoid truncation artifacts and achieve highest resolution, one should sample up to πT_2* of the slowest-decaying signal (31.4 ms). Sampling to 6.4 ms (2x the average T_2*) results in truncation artifacts in the indirect dimension of both US and NUS data by MINT, and moderate *i*SNR gains ca. 1.3 fold (Figure 9ab, Table 1). Similar findings result for sampling to 9.6 ms (Table 1) Yet, sampling to 31.4 ms gives truncation-artifact-free spectra in US and NUS datasets, and yields greater *i*SNR enhancements of 1.7–2 fold (Figure 9cd, Table 1).

The experimentally observed enhancements depend on the maximum evolution time and sampling bias, consistent with the analytic expressions shown in this (Eq. 7ab) and our earlier reports (Eqs. 1–6).[7,12] The US and NUS (50% retained samples) experiments used equal total times, and the NUS followed 35 Hz, 100 Hz, and 300 Hz exponential decays to test different biases (Table 1). The line widths also depend on the maximum evolution time and sampling bias when evolution times are insufficient to overcome the truncation artifacts. (Table 1, example given in Figure S3)

Maximum entropy interpolation (MINT) is a protocol for achieving linear maximum entropy reconstructions of spectra from non-uniformly sampled time domain data.[7] Maximum entropy reconstruction has long been noted for its insensitivity to truncation artifacts,[21] however the linearity of MINT forces spectral reconstructions to closely approximate the behavior of the Fourier Transform, and truncation artifacts arise from applying MINT to severely truncated NUS data as in Figure 9. We further illustrate this concept by contrasting MINT with the more common use of maximum entropy reconstruction in a non-linear regime in Figure 10 (Figure 10a reproduces Figure 10a to facilitate comparisons), and illustrates the application of MINT to a uniformly sampled indirection dimension of ^{13}C-^{13}C correlation spectra in the solid phase, and when the maximum evolution time is just 6.4 ms. Strong truncation wiggles are observed for MINT conditions, achieved by setting the parameter lambda (λ) to very large values in order to force extremely close agreement between mock and experimental time domain samples. Significant truncation wiggles are also observed for MINT processing of uniform data sampled to 9.6 ms (Figure 10b). In contrast Figure 10c illustrates the common application of MaxEnt in which λ is set to intermediate values which deliver high fidelity reconstructions, but which are no longer linear.[21] Truncation artifacts are reduced significantly in Figure 10c, but peak intensities have changed and are no longer linear.

Author Manuscript Author Manuscript Author Manuscript Author Manuscript

Conclusion

Recording the indirect dimensions of nD-NMR by weighted non-uniform sampling is rigorously shown with new theorems to have benefits with respect to the intrinsic SNR and sensitivity of the detected signals. First, and a particularly broad result, any weighting of NUS which has a decreasing probability density always has greater sensitivity than US for recording decaying signals in indirect evolution periods. Both conservative and aggressive NUS densities yield useful sensitivity improvements. Next, the *i*SNR is shown to always increase with evolution time for matched exponential NUS, while many other useful sampling densities have this property as well, bearing the critical implication that *i*SNR and resolution are simultaneously improved with additional evolution time. The results presented here are (i) *intrinsic properties of the raw NUS data*, prior to any signal manipulation and processing, and (ii) applicable to all NUS protocols (off-grid, on-grid, weighted transients, hypercomplex, etc.) that acquire data following a sampling density. These theorems, with broad applicability, assure the performance of widely used approaches to NUS, and it is hoped this work will stimulate its broader adoption.

Supplementary Material

Refer to Web version on PubMed Central for supplementary material.

Acknowledgments

T.P. and C.L.S. acknowledge Agilent for partial support (UCR grant) and NIH (P50GM082251 from NIGMS).

References

1. Barna JCJ, Laue ED, Mayger MRS, Skilling J, Worrall SJP. Exponential sampling, an alternative method for sampling in two-dimensional NMR experiments. J Magn Reson. 1987; 73:69–77.
2. Barna JCJ, Laue ED, Mayger MR, Skilling J, Worrall SJP. Reconstruction of Phase-Sensitive Two-Dimensional Nmr-Spectra Using Maximum-Entropy. Biochem Soc T. 1986; 14:1262–1263.
3. Hoch JC, Maciejewski MW, Mobli M, Schuyler AD, Stern AS. Nonuniform Sampling and Maximum Entropy Reconstruction in Multidimensional NMR. Accounts Chem Res. 2014; 47:708–717.
4. Becker ED, Ferretti JA, Gambhir PN. Selection of Optimum Parameters for Pulse Fourier-Transform Nuclear Magnetic-Resonance. Analytical Chemistry. 1979; 51:1413–1420.
5. Rovnyak D, Hoch JC, Stern AS, Wagner G. Resolution and sensitivity of high field nuclear magnetic resonance spectroscopy. Journal of Biomolecular NMR. 2004; 30:1–10. [PubMed: 15452430]
6. Matson GB. Signal Integration and Signal-to-Noise Ratio in Pulsed Nmr Relaxation Measurements. Journal of Magnetic Resonance. 1977; 25:477–480.
7. Paramasivam S, Suiter CL, Hou GJ, Sun SJ, Palmer M, Hoch JC, Rovnyak D, Polenova T. Enhanced Sensitivity by Nonuniform Sampling Enables Multidimensional MAS NMR Spectroscopy of Protein Assemblies. J Phys Chem B. 2012; 116:7416–7427. [PubMed: 22667827]
8. Palmer, M.; Gupta, RA.; Richard, M.; Suiter, CL.; Hoch, JC.; Polenova, T.; Rovnyak, D. Application of nonuniform sampling for sensitivity enhancement of small molecule heteronuclear correlation NMR spectra. In: Martin, Gary E.; Williams, Antony J.; Rovnyak, David, editors. Modern NMR Approach for the Structure Elucidation of Natural Products. RSC Publishing; 2015. In Press
9. Levitt MH, Bodenhausen G, Ernst RR. Sensitivity of Two-Dimensional Spectra. J Magn Reson. 1984; 58:462–472.

Author Manuscript Author Manuscript Author Manuscript Author Manuscript

10. Kumar A, Brown CB, Donlan ME, Meier BU, Jeffs PW. Optimization of two-dimensional NMR by matched accumulation. J Magn Reson. 1991; 95:1–9.
11. Heise H, Seidel K, Etzkorn M, Becker S, Baldus M. 3D NMR spectroscopy for resonance assignment and structure elucidation of proteins under MAS: novel pulse schemes and sensitivity considerations. Journal of magnetic resonance. 2005; 173:64–74. [PubMed: 15705514]
12. Rovnyak D, Sarcone M, Jiang Z. Sensitivity enhancement for maximally resolved two-dimensional NMR by nonuniform sampling. Magnetic Resonance in Chemistry. 2011; 49:483–491. [PubMed: 21751244]
13. Barna JCJ, Laue ED. Conventional and Exponential Sampling for 2d Nmr Experiments with Application to a 2d Nmr-Spectrum of a Protein. Journal of Magnetic Resonance. 1987; 75:384–389.
14. Schuyler AD, Maciejewski MW, Stern AS, Hoch JC. Formalism for hypercomplex multidimensional NMR employing partial-component subsampling. J Magn Reson. 2013; 227:20–24. [PubMed: 23246651]
15. Qiang W. Signal enhancement for the sensitivity-limited solid state NMR expderiments using a continuous non-uniform acquisition scheme. J Magn Reson. 2011; 213:171–175. [PubMed: 21930405]
16. Waudby CA, Christodoulou J. An analysis of NMR sensitivity enhancements obtained using non-uniform weighted sampling, and the application to protein NMR. J Magn Reson. 2012; 219:46–52. [PubMed: 22609525]
17. Manassen Y, Navon G. Nonuniform Sampling in Nmr Experiments. Journal of Magnetic Resonance. 1988; 79:291–298.
18. Maciejewski MW, Qui HZ, Rujan I, Mobli M, Hoch JC. Nonuniform sampling and spectral aliasing. J Magn Reson. 2009; 199:88–93. [PubMed: 19414274]
19. Schmieder P, Stern AS, Wagner G, Hoch JC. Quantification of maximum-entropy spectrum reconstructions. J Magn Reson. 1997; 125:332–339. [PubMed: 9144266]
20. Paramasivam S, Suiter CL, Hou G, Sun S, Palmer M, Hoch JC, Rovnyak D, Polenova T. Enhanced sensitivity by nonuniform sampling enables multidimensional MAS NMR spectroscopy of protein assemblies. J Phys Chem B. 2012; 116:7416–7427. [PubMed: 22667827]
21. Hoch, JC.; Stern, AS. NMR Data Processing. Wiley; New York: 1996.
22. Rovnyak D, Frueh DP, Sastry M, Sun ZYJ, Stern AS, Hoch JC, Wagner G. Accelerated acquisition of high resolution triple-resonance spectra using nonuniform sampling and maximum entropy reconstruction. Journal of Magnetic Resonance. 2004; 170:15–21. [PubMed: 15324754]
23. Mobli M, Hoch JC. Nonuniform sampling and non-Fourier signal processing methods in multidimensional NMR. Prog Nucl Mag Res Sp. 2014; 83:21–41.
24. Mayzel M, Rosenlow J, Isaksson L, Orekhov VY. Time-resolved multidimensional NMR with non-uniform sampling. Journal of Biomolecular NMR. 2014; 58:129–139. [PubMed: 24435565]
25. Sun S, Gill M, Li Y, Huang M, Byrd RA. Efficient and generalized processing of multidimensional NUS NMR data: the NESTA algorithm and comparison of regularization terms. J Biomol NMR. 2015; 62:105–117. [PubMed: 25808220]
26. Bostock MJ, Holland DJ, Nietlispach D. Compressed sensing reconstruction of undersampled 3D NOESY spectra: application to large membrane proteins. Journal of Biomolecular NMR. 2012; 54:15–32. [PubMed: 22833055]
27. Holland DJ, Bostock MJ, Gladden LF, Nietlispach D. Fast Multidimensional NMR Spectroscopy Using Compressed Sensing. Angewandte Chemie-International Edition. 2011; 50:6548–6551.
28. Hyberts SG, Milbradt AG, Wagner AB, Arthanari H, Wagner G. Application of iterative soft thresholding for fast reconstruction of NMR data non-uniformly sampled with multidimensional Poisson Gap scheduling. Journal of Biomolecular NMR. 2012; 52:315–327. [PubMed: 22331404]
29. Stern AS, Donoho DL, Hoch JC. NMR data processing using iterative thresholding and minimum l(1)-norm reconstruction. Journal of Magnetic Resonance. 2007; 188:295–300. [PubMed: 17723313]
30. Martin GE, Blinov KA, Reibarkh M, Williamson RT. 1JCC-edited HSQC-1,n-ADEQUATE: a new paradigm for simultaneous direct and long-range carbon-carbon correlation. Magnetic Resonance in Chemistry. 2012; 50:722–728. [PubMed: 22996413]

Author Manuscript Author Manuscript Author Manuscript Author Manuscript

31. Blinov KA, Williams AJ, Hilton BD, Irish PA, Martin GE. The use of unsymmetrical indirect covariance NMR methods to obtain the equivalent of HSQC-NOESY data. Magnetic Resonance in Chemistry. 2007; 45:544–546. [PubMed: 17437315]
32. Palmer MR, Wenrich BR, Stahlfeld P, Rovnyak D. Performance tuning non-uniform sampling for sensitivity enhancement of signal-limited biological NMR. J Biomol NMR. 2014; 58:303–314. [PubMed: 24682944]
33. Donoho DL, Johnstone IM, Stern AS, Hoch JC. Does the maximum entropy method improve sensitivity? Proc Natl Acad Sci U S A. 1990; 87:5066–5068. [PubMed: 11607089]
34. Hoch JC, Maciejewski MW, Filipovic B. Randomization improves sparse sampling in multidimensional NMR. J Magn Reson. 2008; 193:317–320. [PubMed: 18547850]
35. Spencer RG. Equivalence of the time-domain matched filter and the spectral-domain matched filter in one-dimensional NMR spectroscopy. Concept Magn Reson A. 2010; 36A:255–265.
36. Ernst, RR.; Bodenhausen, G.; Wokaun, A. Principles of Nuclear Magnetic Resonance in One and Two Dimensions. Oxford University Press; Oxford, UK: 1987.
37. Hyberts SG, Robson SA, Wagner G. Exploring signal-to-noise ratio and sensitivity in non-iniformly sampled multi-dimensional NMR spectra. J Biomol NMR. 2013; 55:167–178. [PubMed: 23274692]
38. Stern AS, Li KB, Hoch JC. Modern spectrum analysis in multidimensional NMR spectroscopy: comparison of linear-prediction extrapolation and maximum-entropy reconstruction. J Am Chem Soc. 2002; 124:1982–1993. [PubMed: 11866612]
39. Suiter CL, Paramasivam S, Hou G, Sun S, Rice D, Hoch JC, Rovnyak D, Polenova T. Sensitivity gains, linearity, and spectral reproducibility in nonuniformly sampled multidimensional MAS NMR spectra of high dynamic range. Journal of Biomolecular NMR. 2014; 59:57–73. [PubMed: 24752819]
40. Takegoshi K, Nakamura S, Terao T. 13C-1H dipolar-assisted rotational resonance in magic-angle spinning NMR. Chem Phys Lett. 2001; 344:631–637.

Appendix I

Theorem I (NUS Sensitivity Theorem)

Assume $h(t)$ is a positive, nonincreasing function on some interval $0 \le t < A$, where $A \le \infty$. For any positive T_2 and $0 < t_{max} < A$, the time domain nSNR enhancement (Eq. 4) satisfies

$$\eta = \frac{\alpha}{(1-e^{-\alpha})} \frac{\int_0^{t_{max}} h(t) e^{-t/T_2}\, dt}{\int_0^{t_{max}} h(t) dt} \ge 1, \quad \text{(A1)}$$

where $\alpha = t_{max}/T_2$, and equality holds in Eqn. (A1) if and only if $h(t)$ is constant for $0 < t < t_{max}$.

Proof

We will prove Eqn. (A1) with strict inequality in the case that is most broadly used in experimentation, namely where $h(t)$ is positive, continuous, and strictly decreasing on the [0,A). Let $v = t/T_2$ and so $dt = T_2 dv$. Also set $k(v) = h(T_2 v)$. The inequality to be proved becomes

$$\eta = \frac{\alpha}{(1-e^{-\alpha})} \frac{\int_0^{\alpha} k(v) e^{-v} dv}{\int_0^{\alpha} k(v) dv} > 1, \quad \text{(A2)}$$

Author Manuscript Author Manuscript Author Manuscript Author Manuscript

where $0 < \alpha < A/T_2$. The denominators in Eq. A2 are positive, so the inequality to be proved is

$$\int_0^\alpha k(v)e^{-v}dv > \frac{1-e^{-\alpha}}{\alpha}\int_0^\alpha k(v)dv, \quad \text{(A3)}$$

or $F(\alpha) > 0$ where

$$F(\alpha) = \int_0^\alpha k(v)e^{-v}dv - \left(\frac{1-e^{-\alpha}}{\alpha}\right)\int_0^\alpha k(v)dv > 0.$$

Notice $F(0) = 0$, and so Eq. A3 will be proved if $F'(\alpha) > 0$, or

$$\frac{d}{d\alpha}\int_0^\alpha k(v)e^{-v}dv > \frac{d}{d\alpha}\left(\frac{1-e^{-\alpha}}{\alpha}\int_0^\alpha k(v)dv\right), \quad \text{(A4)}$$

for all $0 < \alpha < A/T_2$. By the Fundamental Theorem of Calculus, the inequality of A4 becomes

$$\begin{aligned} k(\alpha)e^{-\alpha} &> \left(\tfrac{1-e^{-\alpha}}{\alpha}\right)'\int_0^\alpha k(v)dv + \left(\tfrac{1-e^{-\alpha}}{\alpha}\right)k(\alpha), \text{ or} \\ k(\alpha)\left(e^{-\alpha} - \tfrac{1-e^{-\alpha}}{\alpha}\right) &> \left(\tfrac{1-e^{-\alpha}}{\alpha}\right)'\int_0^\alpha k(v)dv. \end{aligned} \quad \text{(A5)}$$

Notice that

$$\left(\frac{1-e^{-\alpha}}{\alpha}\right)' = \frac{\alpha e^{-\alpha} - (1-e^{-\alpha})}{\alpha^2} = \frac{1}{\alpha}\left(e^{-\alpha} - \frac{1-e^{-\alpha}}{\alpha}\right), \quad \text{(A6)}$$

so that Eq. A5 becomes

$$k(\alpha)\left(e^{-\alpha} - \frac{1-e^{-\alpha}}{\alpha}\right) > \frac{1}{\alpha}\left(e^{-\alpha} - \frac{1-e^{-\alpha}}{\alpha^2}\right)\int_0^\alpha k(v)dv. \quad \text{(A7)}$$

Although the common factor in Eq. A6 can be cancelled, it should be recognized that it is negative:

$$e^{-\alpha} - \frac{1-e^{-\alpha}}{\alpha} < 0.$$

Thus the direction of the inequality in Eq. A7 must be changed when performing the cancellation, yielding the following expression that needs to be proved:

Author Manuscript Author Manuscript Author Manuscript Author Manuscript

$$k(\alpha)<\frac{1}{\alpha}\int_0^\alpha k(v)dv. \quad \text{(A8)}$$

By the Mean Value Theorem, there exists an α_1 in [0,α] such that

$$\int_0^\alpha k(v)dv=(\alpha-0)k(\alpha_1),$$

where $a_1 \neq a$ because $k(v)$ is strictly decreasing. Since then $a_1 < a$, we have $k(a_1)>k(a)$, and then

$$\int_0^\alpha k(v)dv=\alpha k(\alpha_1)>\alpha k(\alpha), \quad \text{(A9)}$$

which proves the inequality of Eq. (A8).

The complete case of Eqn. (A1) for any nonincreasing function can be obtained from the special case proved above by an approximation argument. The main step for the last assertion of the theorem is to show that equality in Eqn. (A1) holds only for constant $h(t)$. A complete proof is provided in the Supplementary Information(S5).

Appendix 2

Theorem 2 (Matched NUS SNR Theorem)

The tSNR of matched exponential NUS (Equation 7b) always has a positive slope for an arbitrary, positive T_2 and positive evolution time t_{max}.

Proof

It is necessary to show that the derivative of equation 7b is positive for $t > 0$,

$$\frac{dt}{dt}SNR_{\mathrm{exp-match}}=\frac{d}{dt}\left(\frac{\sqrt{t}}{2}\left(1+e^{-t/T_2}\right)\right)>0. \quad \text{(A10)}$$

One finds

$$\frac{d}{dt}SNR_{\mathrm{exp-match}}=\frac{1}{4\sqrt{t}}\left(1+e^{-t/T_2}\left(1-\frac{2t}{T_2}\right)\right), \quad \text{(A11)}$$

where the sign of the derivative is positive if

$$w(\alpha)=1+e^{\alpha}(1-2\alpha)>0, \quad \text{(A12)}$$

where $\alpha=t/T_2$. Equation A12 is always positive for $\alpha > 0$, which can be seen as follows. The issue in determining if equation A12 is always positive is that (1–2α) can be negative for

Author Manuscript Author Manuscript Author Manuscript Author Manuscript

physically meaningful values of a. A formal min/max calculation on Eq. A12 is straightforward, and will establish the existence of a positive minimum for equation A12. A more succinct approach is also possible. Notice first that $w(0) = 2$ and $\lim_{a\to\infty} w(a) = 1$. To understand the behavior of $w(\alpha)$ for $0 < a < \infty$ examine the slope of $w(a)$,

$$w'(\alpha) = -e^{-\alpha}(1-2\alpha) + e^{-\alpha}(-2) = e^{-\alpha}(2\alpha-3). \quad \text{(A13)}$$

Equation A13 shows a minimum at $\alpha=3/2$, where the slope is negative for $0 < \alpha < 3/2$, and is positive for $3/2 < \alpha$, establishing $a=3/2$ as a minimum in $w(a)$. We see that

$$w(3/2) = 0.5537\ldots,$$

and so $w(t)$ is always equal or greater than this value and therefore always positive.

Author Manuscript Author Manuscript Author Manuscript Author Manuscript

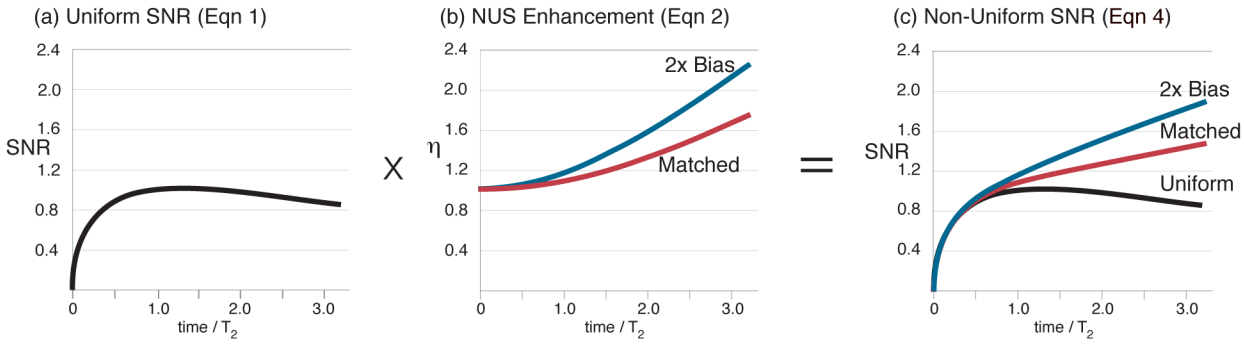

Figure 1.

(a–b) Deriving the *i*SNR of matched and 2X-biased exponential NUS per Eqs. 1–4. (c) The *i*SNR increases monotonically, has no maximum, and is always greater than US. Figures scaled so US to 1.26 T_2 has *i*SNR=1.

Author Manuscript Author Manuscript Author Manuscript Author Manuscript

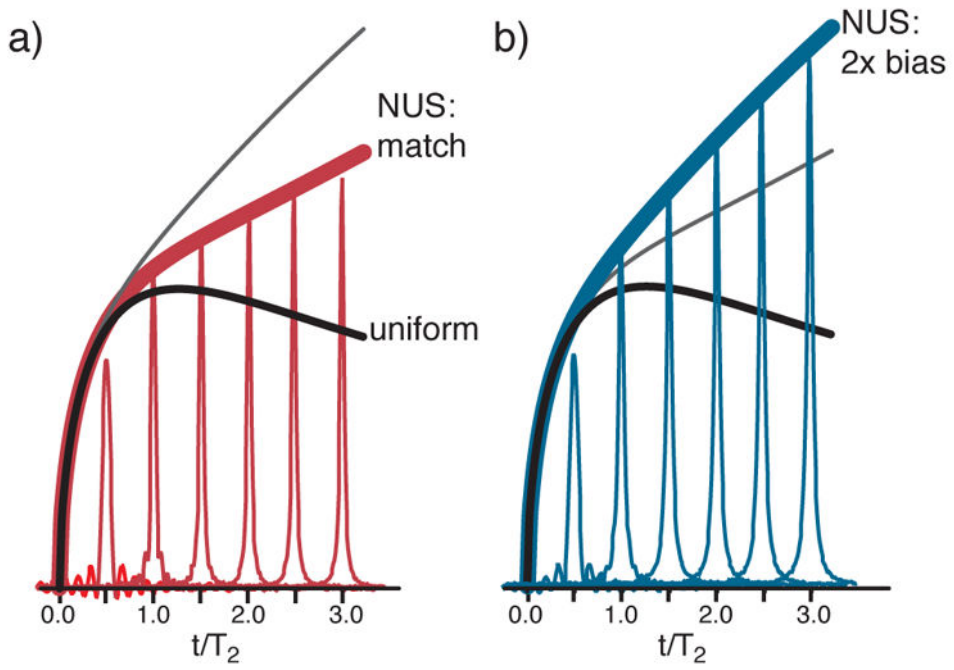

Figure 2.

The *i*SNR of exponential NUS (Eqs. 4–7, Figure 1c) is tested by applying the FFT to a synthetic signal that has non-uniform intensity on the uniform grid injected in to a real noise FID[1]: the resulting peaks are shown for (a) matched (red) NUS and (b) two-fold biased (blue) NUS. These simulated peaks are superimposed on the solid lines that illustrate the formal theoretical predictions given by Eq. 7a for matched(red) and two-fold biased (blue) NUS. The black line corresponds to the *i*SNR of US (Eq. 1).

Author Manuscript Author Manuscript Author Manuscript Author Manuscript

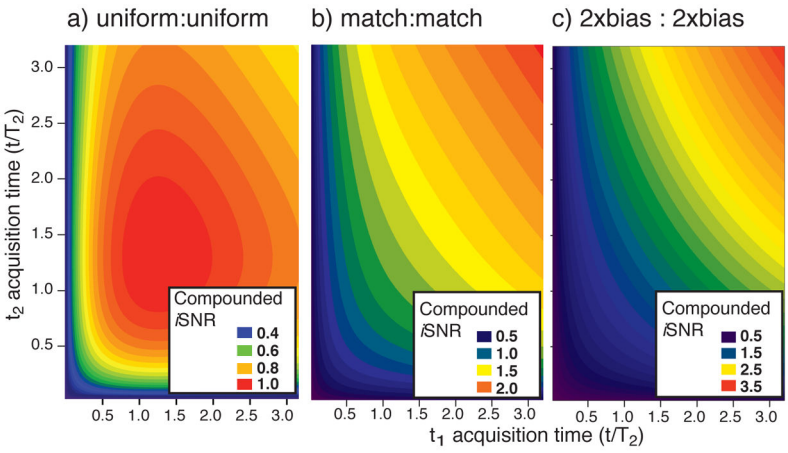

Figure 3.

Representative contour plots delineate the achievable *i*SNR in nD-NMR when (a) US is applied in each of two indirect dimensions and (b–c) NUS is applied in each of two indirect dimensions as a function of acquisition time. Notice the rather steeply decreasing iSNR when both indirect dimensions are sampled by US. In contrast panel (b) shows the *i*SNR when a matched exponential sampling bias is applied in each indirect dimension, and panel (c) shows the iSNR for employing 2x exponentially biased NUS in each indirect dimension. Values are scaled such that uniform acquisition to 1.26 T_2 in both indirect dimensions has a *i*SNR of 1.

Author Manuscript Author Manuscript Author Manuscript Author Manuscript

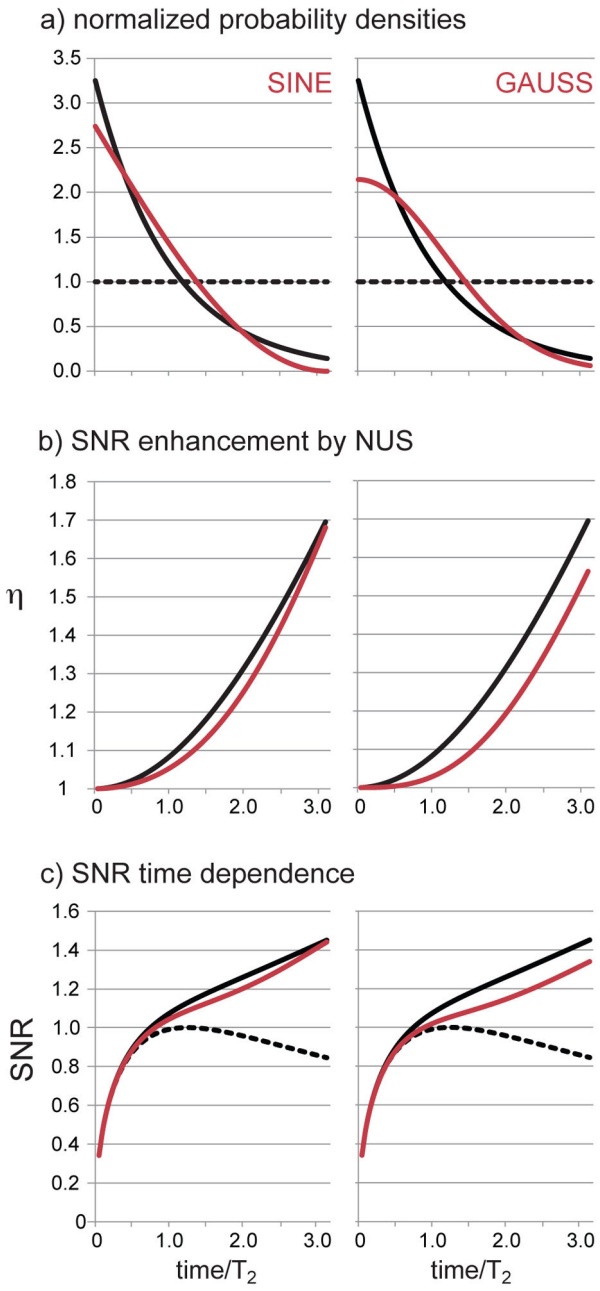

Figure 4.

NUS probability densities following a sinusoid and a Gaussian are analyzed following the same procedure as illustrated for exponential sampling in Figure 1. In all panels, the behavior of matched exponential NUS is given by the solid black line for comparison, while uniform sampling is described by the dashed black line. In (a) the sinusoid and matched exponential densities have been normalized to have the same area as uniform sampling; the value of χ is given by equation 8b or 9b. In (b) the *i*SNR NUS enhancements over US given by equations 8c or 9c are illustrated. In (c) the direct *i*SNR is obtained by multiplying the

Author Manuscript Author Manuscript Author Manuscript Author Manuscript

enhancement in equation 8c (sinusoid) or 9c (Gaussian) by the *i*SNR of uniform sampling in equation 1.

Author Manuscript Author Manuscript Author Manuscript Author Manuscript

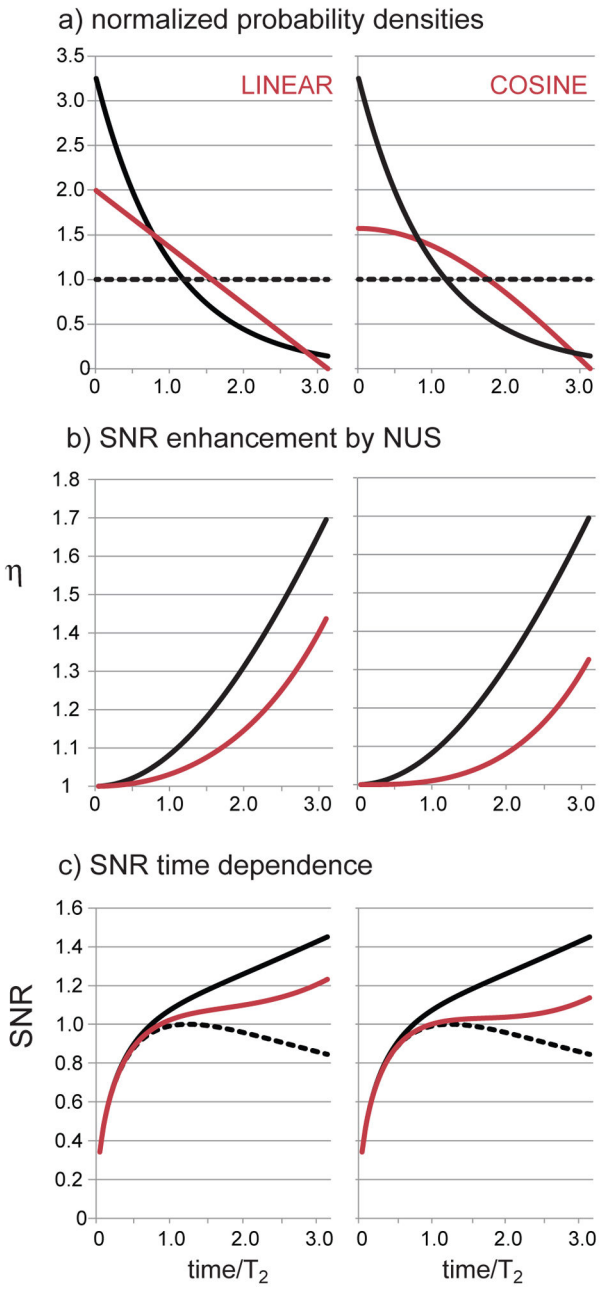

Figure 5.

NUS probability densities following a line and a cosine are analyzed following the same procedure as illustrated for exponential sampling in Figure 1. In all panels, the behavior of matched exponential NUS is given by the solid black line for comparison, while uniform sampling is described by the dashed black line. In (a) the linear and cosine densities have been normalized to have the same area as uniform sampling; the value of χ is given by equation 10b or 11b. In (b) the *i*SNR NUS enhancements over US as given by equations 10c or 11c are illustrated. In (c) the direct *i*SNR is obtained by multiplying the enhancement in equation 10c (sinusoid) or 11c (Gaussian) by the *i*SNR of uniform sampling in equation 1.

Author Manuscript Author Manuscript Author Manuscript Author Manuscript

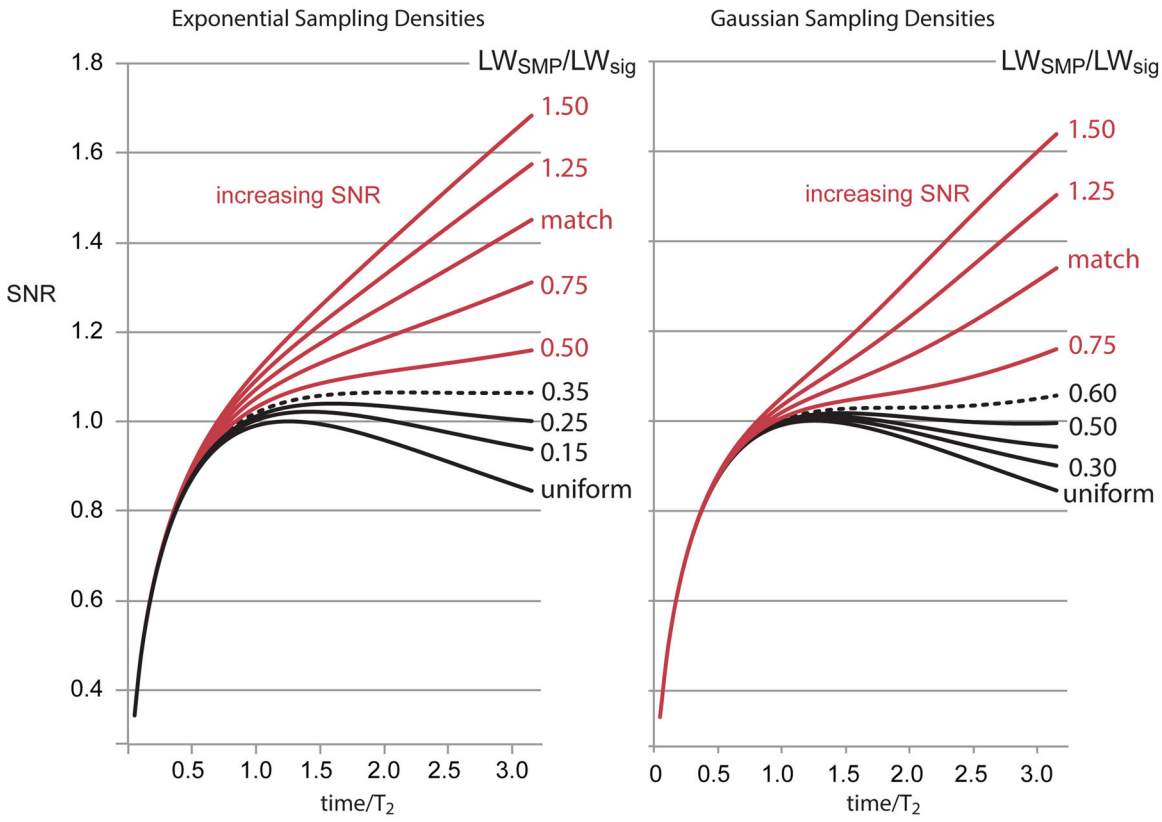

Figure 6.

The time dependence of the *i*SNR is computed for several different cases of exponential and Gaussian NUS applied to an exponentially decaying signal. All cases resulting in a positive *i*SNR slope with evolution time are colored red, showing that broad classes of even very conservative NUS densities possess this critical property. Notice also that all of the exponential and Gaussian densities have *i*SNR greater than uniform sampling, as required by Theorem 1.

Author Manuscript Author Manuscript Author Manuscript Author Manuscript

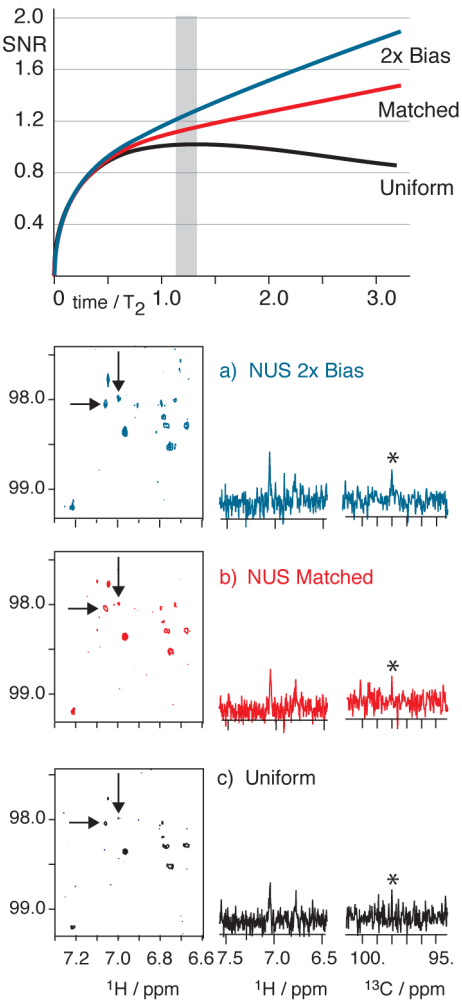

Figure 7.

$^{1}H(^{13}C)$ HSQC spectra of 9 mg natural product spanning an evolution time of about 1.3 T_2. Very little improvement occurs for either matched or two-fold biased NUS as seen in panels (a–c): 3 hrs each, NUS selecting 160 of 640 uniform samples. (US: 4 transients per sample; NUS:16 per sample). Contour levels are consistent in (a–c). All NUS spectra processed by MaxEnt. The *i*SNR in (a–c) was adjusted by mis-setting pulse lengths so that signals by US would be at the limit of detectability; thus the very slight improvement in the ability to distinguish signals by NUS reflects the small iSNR improvement by NUS for evolution times spanning 1.3 T_2. (shaded vertical bar)

Author Manuscript Author Manuscript Author Manuscript Author Manuscript

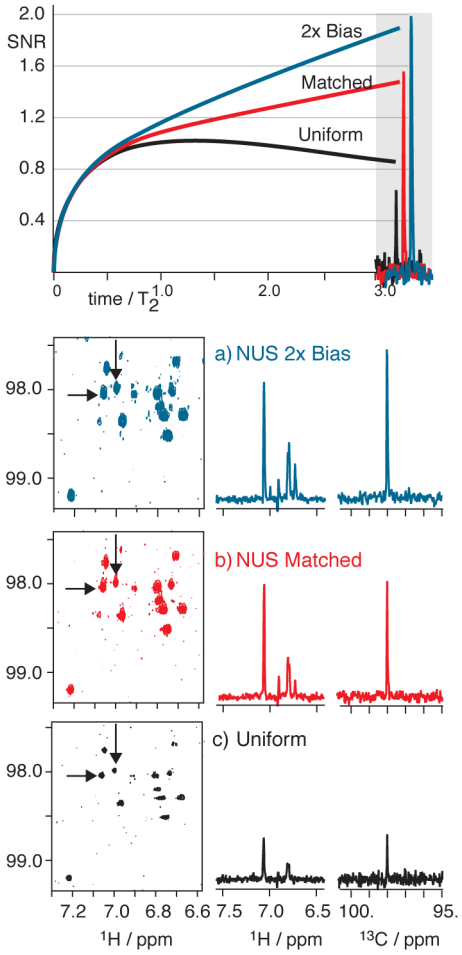

Figure 8.

$^{1}H(^{13}C)$ HSQC spectra of 9 mg natural product spanning an evolution time of about 3 T_2. Significant improvements in signal levels occur for matched or two-fold biased NUS as seen in panels (a–c): 9 hrs each, NUS selecting 400 of 1600 uniform samples. (US: 4 transients per sample; NUS:16 per sample). Contour levels are consistent in (a–c) so that as peaks grow in intensity from (a) to (c) the base of the peak rises above the noise, but the lines are not broadening. Inspection of the ^{13}C cross-sections shows that line widths are not significantly changed from (a) to (c). The ^{13}C cross-sections are overlaid at approximately the 3 T_2 evolution period to show close correspondence to theoretical predictions.

Author Manuscript Author Manuscript Author Manuscript Author Manuscript

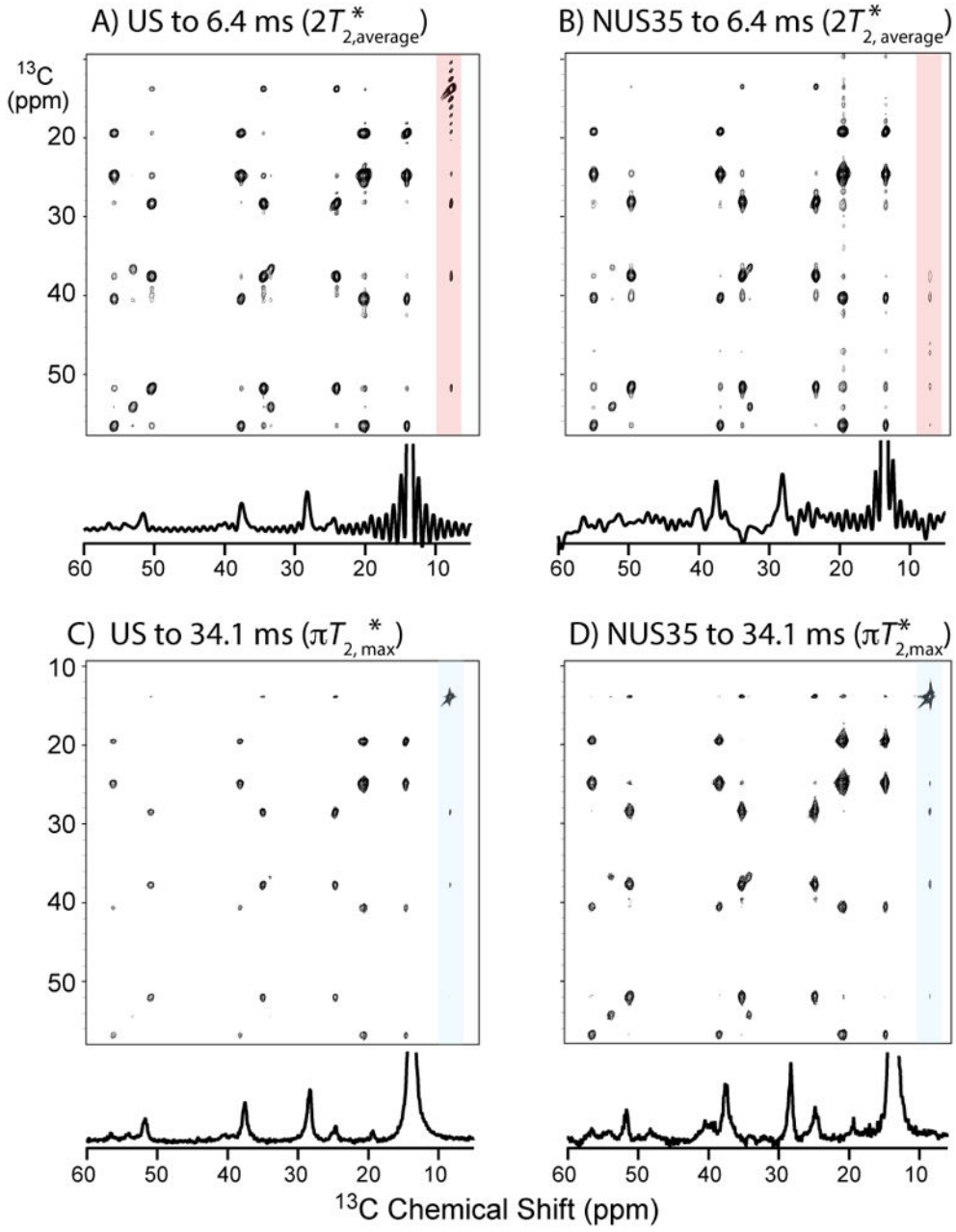

Figure 9.

2D ^{13}C-^{13}C DARR[40] 14.1 T spectra of U-^{13}C,^{15}N-MLF at full spectral width.(Table 1) (A) US/MINT to 6.4 ms in f_1 (2x the average T_2*), (B) NUS35/MINT to 6.4 ms in f_1, (C) US/MINT to 34.1 ms in f_1 (π x longest T_2*), (D) NUS35/MINT to 34.1 ms in f_1. Peaks enhanced more for the 34.1 ms data (same contour levels. For US: 2000x1024 complex, 4 scans per t_1 step, equally spaced by dwell time (33.33 ms) to 6.4, 9.6, or 34.1 ms. For NUS: 2000x512 complex, 8 scans per t_1 step; 512 t_1 samples followed exponential densities of 35 Hz (T_2* of slowest decaying signal; NUS35), 100 Hz (average T_2*; NUS100), or 300 Hz (NUS300) to final samples of 6.4, 9.6, or 31.4 ms.

Author Manuscript Author Manuscript Author Manuscript Author Manuscript

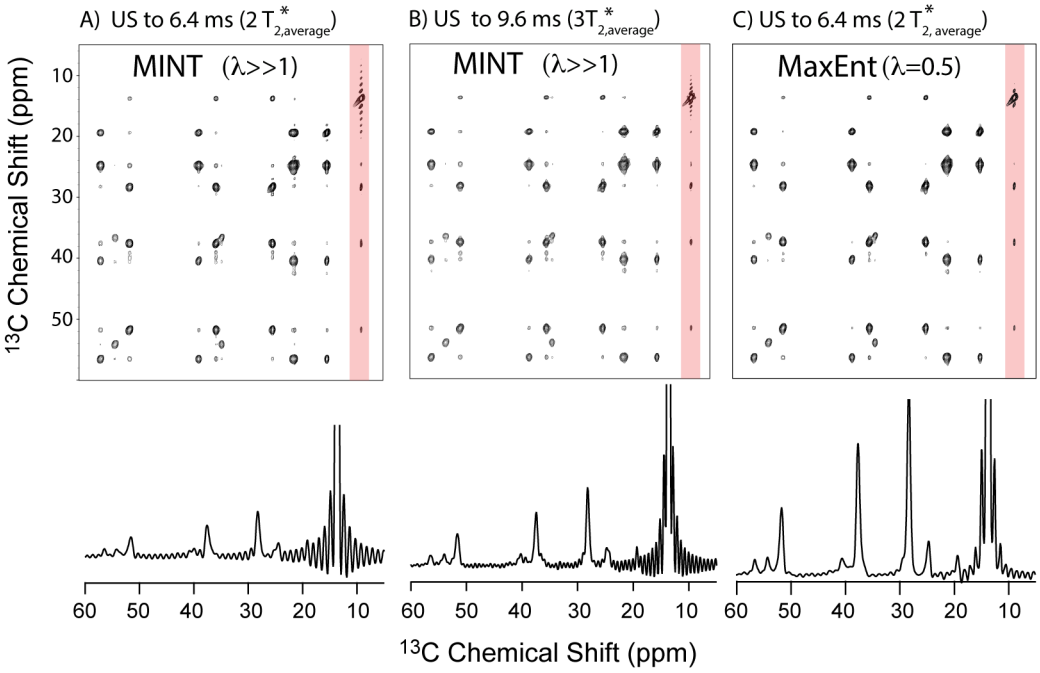

Figure 10.

Comparison of MINT versus traditional non-linear MaxEnt for 2D ^{13}C-^{13}C DARR spectroscopy in MLF (see main text, Figure 4). Figure 9A reproduces Figure 8A. MINT conditions (50% NUS with $\lambda \gg 1$) result in truncation wiggles for truncated signals, however MaxEnt conditions ($\lambda = 0.5$) exhibit significant nonlinearity while also strongly suppressing truncation artifacts, as has been widely described.[21]

Author Manuscript

Author Manuscript

Author Manuscript

Author Manuscript

Table 1

Measured NUS *i*SNR enhancements (η) and average line widths (LW) depend on evolution time.

Experiment	Evolution (ms)*	η (vs. US)	LW (Hz)
US	6.4		128
NUS 35 Hz	6.4	1.32	133
NUS 100 Hz	6.4	1.36	139
NUS 300 Hz	6.4	**1.47**	166
US	9.6		108
NUS 35 Hz	9.6	1.28	114
NUS 100 Hz	9.6	1.31	122
NUS 300 Hz	9.6	**1.67**	141
US	31.4		101
NUS 35 Hz	31.4	1.69	107
NUS 100 Hz	31.4	**2.10**	107

*(6.4 ms $=2T_{2,\mathrm{avg}}$, 9.6 ms$=3T_{2,\mathrm{avg}}$, 31.4 ms$=\pi T_{2,\mathrm{max}}$)